Wlodek, M., Kolasinska-Sojka, M., Wasilewska, M., Bikondoa, O., Briscoe, W., & Warszynski, P. (2017). Interfacial and structural characteristics of polyelectrolyte multilayers used as cushions for supported lipid bilayers. *Soft Matter*, *13*(43), 7848-7855. https://doi.org/10.1039/C7SM01645J

Soft Matter

Accepted Manuscript

This article can be cited before page numbers have been issued, to do this please use: M. Wlodek, M. Kolasiska-Sojka, M. Wasilewska, O. Bikondoa, W. H. Briscoe and P. Warszyski, *Soft Matter*, 2017, DOI: 10.1039/C7SM01645J.

ROYAL SOCIETY OF CHEMISTRY

rsc.li/soft-matter-journal

View Article Online
DOI: 10.1039/C7SM01645J

Soft Matter

ARTICLE

Interfacial and structural characteristics of polyelectrolyte multilayers used as cushions for supported lipid bilayers

Received 00th January 20xx,
Accepted 00th January 20xx

DOI: 10.1039/x0xx00000x

www.rsc.org/

M. Wlodek,[a] M. Kolasinska-Sojka,*[a] M. Wasilewska,[a] O. Bikondoa,[b] W. H. Briscoe[c] and P. Warszynski[a]

Surface properties of polyelectrolyte multilayers (PEMs) obtained *via* sequential adsorption of oppositely charged polyions from their solutions and used as cushion for supported lipid bilayers were investigated. Five types of polyelectrolytes were used: cationic polyethyleneimine (PEI), poly(diallyldimethylammonium) chloride (PDADMAC), and poly-L-lysine hydrobromide (PLL); and anionic polysodium 4-styrenesulfonate (PSS) and poly-L-glutamic acid sodium (PGA). Wettability and surface free energy of the PEMs were determined by contact angle measurements using the sessile drop analysis. Electrokinetic characterisation of the studied films was performed by streaming potential measurements of selected multilayers and the structure of polyelectrolyte multilayer was characterized by synchrotron X-ray reflectometry. The examined physicochemical properties of PEMs were correlated with the kinetics of the formation of supported lipid bilayers atop the PEM cushion.

1. Introduction

Fabrication of well-defined nanostructures is one of the conditions to obtain nanocomposite materials with novel functions. In 1966 Iler reported the multilayers of colloidal species obtained by sequential adsorption of oppositely charged particles, thereby introducing the Layer-by-Layer (LbL) technique.[1] Decher et al.[2-5] further developed the Layer-by-Layer, showing its great potential for surface modification and functionalization. The LbL mechanism is governed by electrostatic interactions between neighbouring layers and the entropy gain accompanying the counterion release. Possibility of combining various polyelectrolytes (or other nano-objects possessing surface charge) and the sequential build-up procedure allows precise and tuneable structure formation on the nanoscale to introduce desired functions/properties.[5,6] Thus, its simplicity, universality and the high quality of obtained films make the LbL an attractive method for the production of stratified thin films, in which layers are organized in a specifically predetermined order.[7] It leads to a broad range of applications including (bio)sensing,[8] (bio)electronics, targeted delivery of active agents,[9] protein adsorption,[5,10] antimicrobial coatings,[11] tissue engineering,[12] implants, adhesives, catalysis,[13] separation, storage and conversion of energy.[14] The polyelectrolyte film architecture and properties such as thickness, roughness, wettability, solvent responsiveness, surface charge and permeability are controlled by many parameters, which enable the design of appropriate, desired structures. Some key parameters include the polyelectrolyte type, ionic strength, pH and temperature in the solution, type of electrolyte used, deposition time, number of steps during the sequential adsorption, etc.[5] Different experimental techniques have been used to study PEM properties, such as quartz crystal microbalance QCM,[15] surface plasmon resonance (SPR) spectroscopy,[16] ellipsometry,[17] X-ray reflectometry (XRR),[18] neutron reflectometry (NR),[19] atomic force microscopy (AFM),[20] Fourier transform infrared (FTIR) spectroscopy, optical waveguide lightmode spectroscopy (OWLS), etc..[5,12,14] These advantages of PEMs make them a promising candidate as a support for lipid bilayers.[21] Supported lipid bilayers (SLBs) are widely utilized as model cell membranes,[23,24] and in biosensors where they provide a biologically mimicking environment for functional biomolecules such as proteins with sensing activities,[25] interfacing artificial materials with biological system.[22] Lipid bilayer membranes supported on PEMs are also appropriate candidates for dispersed drug delivery systems in particularly for targeted nanoparticle delivery.[26-28]

Using quartz crystal microbalance with monitoring dissipation (QCM-D), we have recently studied adsorption and rupture kinetics of mixed liposomes of 1-palmitoyl-2-oleoyl-sn-glycero-3-phosphocholine/-palmitoyl-2-oleoyl-sn-glycero-3-phosphoethanolamine (POPC/POPE) to form supported lipid bilayers on three polyelectrolyte cushions, each consisting of three layers of two oppositely charged polyelectrolytes atop a

[a] Jerzy Haber Institute of Catalysis and Surface Chemistry, Polish Academy of Sciences Niezapominajek 8, 30-239 Krakow, Poland.
[b] XMas, The UK-CRG Beamline, The European Synchrotron (ESRF), 71 Avenue des Martyrs, 38043 Grenoble, France. Department of Physics, University of Warwick, Gibbet Hill Road, Coventry CV4 7AL, UK.
[c] School of Chemistry, University of Bristol, Cantock's Close, Bristol BS8 1TS, United Kingdom.

View Article Online
DOI: 10.1039/C7SM01645J

PEI layer: $PEI(PSS/PEI)_3$, $PEI(PSS/PDADMAC)_3$, $PEI(PGA/PLL)_3$. Fig. 1 shows the QCM frequency and dissipation shifts upon POPC/POPE deposition on the PEM supporting cushion. A well-established minimum in the frequency shift (Fig. 1A) and a maximum in the energy dissipation (Fig. 1B) indicate that an SLB was formed (at least to some extent) on all the multilayer cushions, but the kinetics and the final structure of obtained bilayers differed on different cushions. The kinetics of liposomes deposition as indicated by the slopes of the initial frequency shift decay and the initial energy dissipation increase in Fig. 1A and B respectively was similar for all the studied cases. However, the critical liposome coverage as indicated by the depth of the frequency shift minima and the dissipation maxima varied. The smallest amount of liposome adsorption to reach the critical coverage (ca. -110Hz) was found on $PEI(PGA/PLL)_3$, the intermediate amount on $PEI(PSS/PDADMAC)_3$ (ca. -150Hz), and the biggest amount on $PEI(PSS/PEI)_3$ (ca. -190Hz). The kinetics of the fusion and rupture step as well as the release of water, as indicated by the shape of the curves after the minima and the maxima, also differed among the studied substrates. Thus, these results show that the amount of liposomes adsorbed, the kinetics of liposome fusion and rupture, as well as the final structure and amount of the obtained SLBs depended on the PEM cushion type, demonstrating the important role of the PEM properties in the SLB formation *via* vesicle fusion.[20]

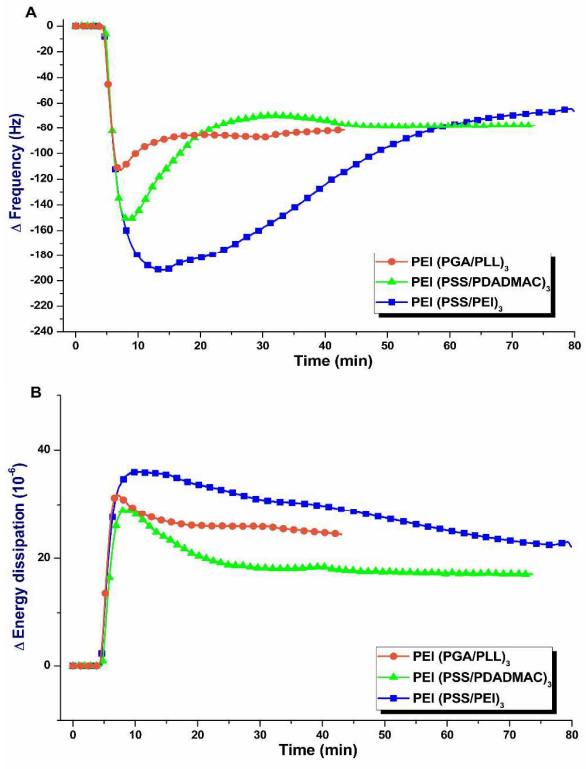

Fig. 1. Comparison of QCM-D frequency shift (A) and energy dissipation (B) due to adsorption and rupture of POPC/POPE liposomes for form lipid bilayers on the polyelectrolyte cushions: $PEI(PGA/PLL)_3$, $PEI(PSS/PDADMAC)_3$, $PEI(PSS/PEI)_3$. Adapted with the permission from [20]. Copyright 2015 American Chemical Society.

Our findings are in agreement with a number of previous studies. Renner et al.[29] found that the degree of hydrophobicity and swelling of the anionic polymer cushions determined both the kinetics of the membrane formation and the mobility of the obtained SLB. Nakamura et al.[30] and Tero et al.[31] found that lipid bilayer formation was affected by the physical and chemical properties of the substrate surface, such as its chemical termination. Additionally, Kim et al.[32] demonstrated the role of the substrate surface charge in supported lipid bilayer formation. These findings have motivated us to further characterise physicochemical properties of polyelectrolyte multilayers in this study and correlate them with supported lipid bilayer formation due to interactions between PEMs and lipids.

An important parameter that controls liposome adhesion is the surface free energy (SFE) of the SLB support, which can be determined by contact angle measurements (e.g. using the sessile drop profile analysis),[33,34] as wetting characteristics provides information on the interactions between solid surfaces and liquids. There are many examples of surface free energy determination for various solid materials, e.g. using Wu,[35] van Oss,[36] Owens-Wendt-Rebel-Kaelble[37-39] or Fowkes[40] models. These approaches are based on measurements of contact angles of different liquids that meet certain preconditions on the same solid sample. For instance, in the methods by Owens and co-workers[38] or Wu,[35] liquids of known values of dispersive and polar components of surface tension are applied. Such SFE measurements are also useful to processes such as Microcontact printing of PEM thin films.[41] As the electrostatic interactions between PEMs and lipids play an important role in liposome deposition on PEMs,[42] surface charge of the polyelectrolyte cushion needs to be characterized. The streaming potential method is useful for assessing electrokinetic properties (zeta potential) of polyelectrolyte films, and their formation and stability on solid supports. The influence of pH, ionic strength and electrolyte composition on PEMs' stability can be studied *in situ*.[43,44] Most frequently the electrokinetic experiments have been carried out using parallel-plate channel cells developed by van Wagenen and Andrade.[45] Scales et al.[46] determined electrokinetic characteristics of bare mica and bare silica surfaces using this setup. Similarly, Adamczyk et al.[47] studied the formation of polyallylamine hydrochloride (PAH)/ polysodium 4-styrenesulfonate (PSS) multilayers on mica, demonstrating that streaming potential method is a sensitive tool for characterizing electrokinetic properties of polyelectrolyte layers. In addition, adsorption of colloidal particles[48] and proteins to surfaces have also been investigated using the streaming potential cell equipped with the parallel-plate channel.[49] For instance, Adamczyk et al.[50] detected the presence of trace amounts (bulk concentration below 10^{-10}M) of adsorbed PAH on mica surface. Norde and Rouwendal determined changes in the streaming potential of glass slides caused by adsorption of lysozyme.[51] Adsorption of BSA (bovine serum albumin) and IgG (immunoglobuline G) was also investigated.[52] Streaming potential measurements were also

View Article Online
DOI: 10.1039/C7SM01645J

performed for fibrinogen adsorption using the parallel-plate channel formed between two mica plates.[53]

To address the above-mentioned factors such as surface charge and hydrophilicity of PEM cushions that affect formation of supported lipid bilayers, in this work we have focused on characterising wetting, surface free energy and zeta potential of a number of PEMs. Furthermore, the structure of PEMs was also characterized by X-ray reflectometry (XRR), which has been used to characterise soft nanofilms[54-55] and previously used to characterise PEMs.[18] XRR can yield useful structural details on the thickness, roughness and electron density, which could be correlated with the physical density of PEMs. Such detailed comparisons of the physicochemical properties of the polyelectrolyte multilayers facilitate understanding how they interact with the species they are exposed to, such as lipid vesicles. Such knowledge is important to controlling the transformation of vesicles in solution into a continuous and stable supported lipid bilayer on a surface for surface functionalization.

2. Materials and Methods

2.1 Materials and sample preparation

The polyelectrolytes used in our studies were: branched poly(ethyleneimine) (PEI), of molecular weight of 750kDa, poly(diallyldimethylammonium)chloride (PDADMAC) in the range of 100-200kDa, (poly-L-lysine hydrobromide) PLL of 30kDa as polycations, and polysodium 4-styrenesulfonate (PSS) of 70kDa, (poly-L-glutamic acid sodium salt) (PGA) of 50kDA as polyanions. All polyelectrolytes were purchased from Sigma-Aldrich. Fig. 2 illustrates their chemical structures. Sodium chloride and diiodomethane, NaOH and HCl of analytical grade were purchased from of Sigma-Aldrich. Ultrapure Millipore water with resistivity >18MΩ cm was used for the preparation of all solutions. Silicon wafers with orientation 100°±0.5° were purchased from On Semiconductor, Czech Republic. Before use, silicon wafers were cleaned with piranha solution, which is a mixture of equivalent volumes of concentrated sulfuric acid and perhydrol (*Precaution! This solution is a very strong oxidizing agent and should be handled carefully*) then rinsed with distilled water and soaked for 30min in hot water (70°C). Deposition of polyelectrolytes by the LbL technique onto silicon wafers was performed from the solution of polyion concentration equal to 0.5g/l and ionic strength of 0.15M NaCl. PDADMAC and PSS were used in their natural pH, since they are strong electrolytes, which mean that they are completely charged over the whole pH range. PLL solution was adjusted to pH=10 to partially reverse its dissociation. Zeta potential of PLL at pH=10 was 12mV. As a reference value, zeta potential of fully charged PLL in acidic condition was ca. 23mV. PGA was used at pH=6, being fully charged with zeta potential equal to -30mV. PEI was used in its natural pH equal to 10.5, at which it is partially dissociated, similarly to PLL. PEI was always used as the first, anchoring layer for the build-up of cushion films.[17] The polyelectrolyte solutions were freshly prepared before each film deposition experiment. Each polyion adsorption step took 10min followed by three times rinsing for 1min in water. The process was continued up to 7-layer film, since in our previous studies we established that for polyelectrolyte multilayers formed in similar conditions 7 layers are sufficient for their surface properties become independent of the solid substrate.[17]

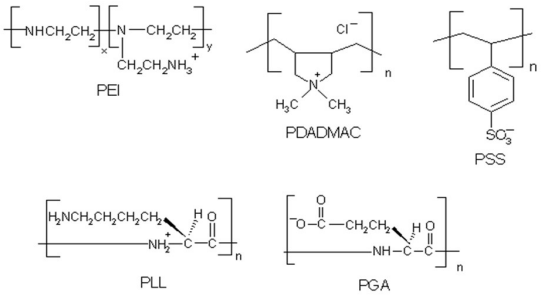

Fig. 2. Chemical structures of polyelectrolytes used.

2.2 Experimental techniques

2.2.1 Contact angle measurements (CA)

The wettability was determined experimentally by contact angle measurements of water and diodomethane droplets on substrates covered with PEMs. Measurements were made using the Drop Shape Analysis System DSA 100M from KRÜSS GmbH. Liquid droplets of 0.03ml in volume were slowly formed at the tip of the pipette and placed on the studied surfaces. The measurements were carried out in the thermostated chamber (25°C) with regulated humidity to prevent drop evaporation, and a CCD camera recorded the image of the sessile drop. The value of the equilibrium contact angle was obtained by fitting the solution of the Young-Laplace equation to the drop shape and calculating the slope of the profile derivative at the three phase contact points. More detailed description of the technique was presented in our previous paper.[34]

2.2.2 Surface free energy (SFE) determination

For the determination of surface free energy of PEMs, water and diiodomethane were used as measuring liquids. For each sample three to five contact angle measurements with either liquid were performed at various locations on the PEMs surface. For calculating the SFE, the Owens-Wendt approach was used, according to the following formulas,

$$(\gamma_{Sd}\gamma_{Wd})^{0.5} + (\gamma_{Sp}\gamma_{Wp})^{0.5} = 0.5\gamma_W(1+\cos\theta_W) \quad (1)$$

$$(\gamma_{Sd}\gamma_{Dd})^{0.5} + (\gamma_{Sp}\gamma_{Dp})^{0.5} = 0.5\gamma_D(1+\cos\theta_D) \quad (2)$$

$$\gamma_S = \gamma_{Sp} + \gamma_{Sd} \quad (3)$$

where the subscript W refers to water as a polar liquid, and D to diiodomethane as a dispersive liquid; γ_S, γ_{Sd} and γ_{Sp} are the calculated SFE value and its polar and dispersive components of the solid, respectively; γ_L, γ_{Ld} and γ_{Lp} are the known SFE value and its polar and disperse components of the measuring liquid, respectively (with L referring to either W or D); and θ is

View Article Online
DOI: 10.1039/C7SM01645J

the contact angle. The following literature values were used: γ_{Wd}=21.8mJ/m^2 and γ_{Wp}=51.0mJ/m^2 for water, and γ_{Dd}=50.8 mJ/m^2 and γ_{Dp}=0.0mJ/m^2 for diiodomethane.[56]

2.2.3 Streaming potential measurements

The zeta potential (ζ) of the PEMs was determined *via* streaming potential measurements using a custom-designed cell described in detail previously.[48] The main part of the cell was a parallel-plate channel of dimensions $2b_c \times 2c_c \times L = 0.027 \times 0.29 \times 3.5$cm, formed by silicon plates separated by a perfluoroethylene spacer. Fluid flow in the channel was gravity induced, i.e. its velocity was controlled by the difference in the hydrostatic pressure ΔP. The streaming potential (E_s) was measured by a pair of Ag/AgCl electrodes for various pressures to obtain the slope of the E_s vs. ΔP dependence. The cell electric resistance Re was determined by using a pair of Pt electrodes to account for the surface conductivity effect. Knowing the slope of the E_s vs. ΔP dependence, one can calculate the apparent zeta potential of the channel surfaces using the Smoluchowski relationship,

$$\xi = \frac{\pi\eta}{\varepsilon}\frac{E_s}{\Delta P}\frac{1}{R_c}\frac{L}{bc} = \frac{4\pi\eta}{\varepsilon}\frac{E_s}{\Delta P}\lambda_{eff} \quad (4)$$

where *L*, *b*, and *c* are the length, thickness, and width of the channel; η is the dynamic viscosity of the solution; ε is the dielectric permittivity; and R_c is the ohmic cell resistance incorporating the surface conductivity effect which can be expressed *via* the effective conductance of electrolyte in the channel $\lambda_{eff.}$ Using these data, one can estimate the effective surface charge density of the polyelectrolyte multilayers by applying the Gouy-Champan formula,[47,53]

$$\sigma_0 = \left(\frac{\epsilon kT\kappa}{4\pi e}\right) sinh\left(\frac{\xi e}{2kT}\right) \quad (5)$$

where k is the Boltzmann constant, T is the absolute temperature, e is the elementary charge and κ^{-1} is the Debye screening length,

$$\kappa^{-1} = \left(\frac{\epsilon KT}{8\pi e^2 I}\right)^{1/2} \quad (6)$$

with I the ionic strength.

2.2.4 Synchrotron X-ray reflectometry (XRR) measurements

The XRR measurements[54-55,57] were performed at beamline BM28 at the European Synchrotron Radiation Facility (ESRF), Grenoble, France. The BM28 monochromator was tuned to select an X-ray beam energy of 14keV with a corresponding wavelength λ=0.886Å. The incident beam size defined by slits was 100μm (vertical) and 240μm (horizontal). The XRR measurements were carried out for all polyelectrolyte multilayers in air at room temperature. In each measurement, a monochromatic incident X-ray beam struck the sample surface at some known grazing angle θ_i (varying from 0.06° to 2.4/2.6°), corresponding to a range (0.014-0.6Å^{-1}) of the vertical momentum transfer vector Q (=4πsin(2θ_i/2)/λ). The specularly reflected intensity was detected at each angle $\theta_r = \theta_i$ using an avalanche photodiode detector (APD). The measured reflectivity curves were analyzed by applying a standard fitting program Motofit[58] in IGOR Pro (WaveMetrics, Portland, USA). The obtained reflectivity curves were optimised by the least χ^2 method by applying the Parrat algorithm as implemented in Motofit, in which the PEMs on PEI coated silica were treated a slabs of different scattering densities. The obtained fitting parameters, i.e. the film (slab) thickness, interfacial roughness, and electron density along the normal to the film allowed us to extract structural information of the PEMs.

3. Results and discussion

Contact angle (CA) and surface free energy (SFE)

We determined the contact angles of water droplets on the substrates covered with polyelectrolyte multilayers as a measure of PEM hydrophobicity. Their values for selected PE films are presented in Table 1.

Table 1 Average contact angle values for water on studied PEMs.

Positively terminated multilayers		Negatively terminated multilayers	
PEI(PGA/PLL)$_3$	 29°±4°	PEI(PGA/PLL)$_3$PGA	 25°±1°
PEI(PSS/PDADMAC)$_3$	 31°±2°	PEI(PSS/PDADMAC)$_3$PSS	 23°±2°
PEI(PSS/PEI)$_3$	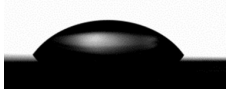 49°±7°	PEI(PSS/PEI)$_3$PSS	 39°±5°

View Article Online
DOI: 10.1039/C7SM01645J

Soft Matter

ARTICLE

All the films terminated by polycations appeared more hydrophobic than polyanion terminated ones, which is a general phenomenon known as the odd-even effect first reported by Hsieh et al.[59] We have also observed it previously with other multilayer systems.[34,60] One can observe from the contact angle values that the PEI-PSS systems - either polycation terminated ($PEI(PSS/PEI)_3$) or polyanion terminated ($PEI(PSS/PEI)_3PSS$ - were more hydrophobic compared to $PEI(PGA/PLL)_3$ and $PEI(PSS/PDADMAC)_3$ with a contact angle difference of ca. 15-20°. Strikingly, PSS as an outermost layer of the film with PDADMAC used as the polycation exhibited a contact angle value ° lower than that in the case of PEI as the polycation. It highlights the impact of the interpenetration of oppositely charged polyions on the surface properties of the resulting PEM film. Table 2 summarizes the total surface free energy (γ_S) its polar (γ_{Sp}) and dispersive (γ_{Sd}) components for various PEMs, obtained using the Owens-Wendt approach as described in the *Materials and Methods* section.

Table 2 The total surface free energy (γ_S) with its polar (γ_{Sp}) and dispersive (γ_{Sd}) components and contact angles of water (θ_W) and diiodomethane (θ_D) on different PEMs.

Positively terminated multilayers					Negatively terminated multilayers				
γ_S	γ_{Sd}	γ_{Sp}	θ_W	θ_D	γ_S	γ_{Sd}	γ_{Sp}	θ_W	θ_D
$PEI(PGA/PLL)_3$					$PEI(PGA/PLL)_3PGA$				
73.7±1.8	48.8±0.3	24.8±1.6	29±4	16±1	75.5±0.5	49.1±0.2	26.4±0.3	25±1	15±1
$PEI(PSS/PDADMAC)_3$					$PEI(PSS/PDADMAC)_3PSS$				
73.0±1.1	49.1±0.5	23.9±0.7	31±2	15±2	76.4±0.8	49.5±0.2	26.9±0.6	23±2	13±1
$PEI(PSS/PEI)_3$					$PEI(PSS/PEI)_3PSS$				
64.0±3.5	49.1±0.2	14.9±3.3	49±7	15±1	69.5±2.5	50.1±0.2	19.6±2.3	39±5	9±1

Practically no differences in the dispersive contribution to the surface free energy are observed for all the films. On the other hand, the polar contribution to γ_S for $PEI(PSS/PEI)_3$ is ca. 60% lower for positively terminated multilayer and ca. 40% lower for negatively terminated film compared to $PEI(PGA/PLL)_3$ and $PEI(PSS/PDADMAC)_3$.

Considering the results for supported lipid bilayer formation on the top of $PEI(PGA/PLL)_3$, $PEI(PSS/PDADMAC)_3$ and $PEI(PSS/PEI)_3$ discussed previously[20] and in the Introduction section, we can correlate the capacity of the SLB formation with the polar component of the surface free energy of polyelectrolyte cushion. While the kinetics of liposome deposition is the same for all the studied PEM supports (Fig. 1), the critical liposomal coverage on $PEI(PSS/PEI)_3$ is much higher than on other PEMs and, on the other hand, the kinetics of vesicle fusion is much slower. It means that a lower γ_{Sp} value inhibits liposome rupture, presumably due to higher vesicle mobility at more hydrophobic, weakly interacting surfaces. In contrast, a higher γ_{Sp} value induces faster liposome rupture. This is in agreement with the study by Isono et al.[61] who found that hydrophilic surfaces were more suitable for uniform supported lipid bilayer formation than hydrophobic surfaces. They explained that the presence of thin (around ne monolayer) film of bound water with much smaller mobility than bulk water promoted lipid deformations, and the deformed vesicles would rupture more easily due to a bigger curvature around their edge. In the case of hydrophobic surfaces, the interface energy between the substrate surface and the vesicle was large, which reduced the interface area. Thus, the vesicles maintained their spherical shape, making vesicle rupture more difficult.[61] However, other studies show stabilization of liposomes by PLL,[62] suggesting that strong interactions between lipids and PLL would result in vesicle adsorption without fusion. We have also observed this behaviour in the case of the formation of POPC/POPE supported lipid bilayer with hydrophobic quantum dots (QDs) on PLL terminated polyelectrolyte films.[63] In that case, the presence of QDs may be an important factor affecting the stability of liposomes. The final lipid layer structure on the PEM cushion was an interplay between the interactions of liposomes with the support and other interactions among lipid molecules within liposomes which are affected by the presence of QDs.[63]

Streaming potential

The zeta potential data for films terminated either by polycations or polyanions is listed in Table 3. Multilayers with polycations as the outermost layer showed similar zeta potential values. For negatively terminated PEMs, a much bigger difference in zeta potential values was observed, and

View Article Online
DOI: 10.1039/C7SM01645J

the magnitude of the differences depended on the type of the PEM film. Surprsingly, films terminated with PSS exhibited different values of zeta potential depending on the type of polycation used for the film build-up. As such, the impact of all the components of the PEM film and their interpenetration, rather than only the outermost layer, on the overall PEM surface property is evident. One should keep this in mind while designing PEMs for specific purposes, that is, its surface properties are controlled by all the polyions and their interactions. These results also suggest that the zeta potential of polyelectrolyte cushions played a secondary role in the bilayer formation, since the adsorption kinetics was different on the PEM cushions with similar zeta potentials (cf. Table 3).

Table 3 Zeta potential and charge density of studied PEMs.

Positively Terminated Multilayers		Negatively Terminated Multilayers	
Zeta Potential (mV)	*Charge density ($e \cdot nm^2$)*	*Zeta Potential (mV)*	*Charge density ($e \cdot nm^2$)*
$PEI(PGA/PLL)_3$		**$PEI(PGA/PLL)_3PGA$**	
24±3	0.036	-20±4	-0.029
$PEI(PSS/PDADMAC)_3$		**$PEI(PSS/PDADMAC)_3PSS$**	
29±2	0.044	-34±3	-0.053
$PEI(PSS/PEI)_3$		**$PEI(PSS/PEI)_3PSS$**	
27±3	0.040	-14±1	-0.020

X-ray reflectivity (XRR)

The XRR curves with best fits using a three layer model (SiO_2/PEI/PEM atop Si) for the three polycation-terminated PEMs, i.e. $PEI(PGA/PLL)_3$, $PEI(PSS/PDADMAC)_3$, $PEI(PSS/PEI)_3$, are shown in Fig. 3. Evident from the different magnitude and spacing of the Kiessig fringes in the XRR curves, PEMs differed in their structures. The fringes are the most pronounced in the case of $PEI(PSS/PDADMAC)_3$. In contrast, the reflectivity curve of $PEI(PGA/PLL)_3$ exhibits very mild fringes, with a larger *Q* fringe spacing, which indicates a rougher and thinner interfacial layer. In the case of $PEI(PSS/PEI)_3$, the fringes are intermediate between the other two PEM systems.

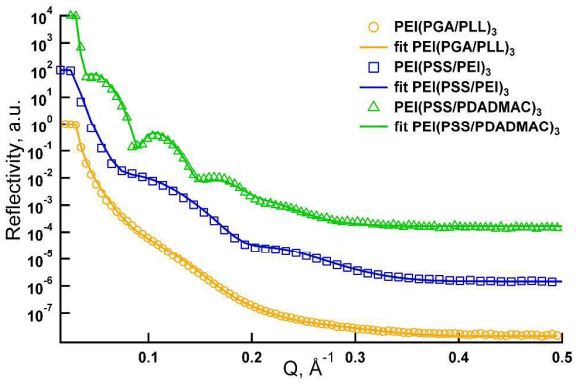

Fig. 3. X-ray reflectivity experimental curves with fits for of $PEI(PGA/PLL)_3$, $PEI(PSS/PEI)_3$, $PEI(PSS/PDADMAC)_3$.

Basing on fitting parameters, i.e. thickness, scattering length density (SLD) and roughness summarized in Table 4, the electron density profiles of the multilayer films have been calculated and are depicted in Fig 4.

Table 4 Best fit parameters to the experimental data given in Figure 3. The fit is based on a three layer model.

Type of PEMs	Thickness (nm)	SLD ($\times 10^{-6}$ Å^{-2})	Roughness (nm)
$PEI(PGA/PLL)_3$	3.3	8.25	2.1
$PEI(PSS/PDADMAC)_3$	9.2	9.97	1.5
$PEI(PSS/PEI)_3$	3.8	6.76	1.1

The fits confirm the above qualitative interpretation of the Kiessig fringe features in the XRR curves. $PEI(PSS/PDADMAC)_3$ shows a thickness of 9.2nm, which is more than twice that for $PEI(PSS/PEI)_3$ (3.8nm) and ~ three times the thickness of $PEI(PGA/PLL)_3$ (3.3nm). The PEM film roughness has similar values for $PEI(PSS/PEI)_3$ and $PEI(PSS/PDADMAC)_3$. However, in the case of $PEI(PGA/PLL)_3$, the roughness is more than 60% of its thickness (in contrary, for $PEI(PSS/PDADMAC)_3$ it is ca. 16%). This is a result of the difficulty in fitting the XRR curve with mild Kiessig fringes. The SLD profiles in Fig. 4 show that $PEI(PSS/PEI)_3$ is not uniform in contrast to well structured $PEI(PSS/PDADMAC)_3$. In relation to the adsorption kinetics of liposomes on these films, this suggests that the PEM roughness can influence bilayer formation. The kinetics of liposome deposition was the same for all studied cases till the maximal liposome coverage was reached (Fig. 1), but differences in kinetics were visible after this. While on the relatively smooth $PEI(PSS/PDADMAC)_3$ vesicle fusion occurred in ca. 10minutes after reaching the critical liposomal coverage, on the relatively rough surface of $PEI(GA/PLL)_3$ film (with the same surface free energy components as $PEI(PSS/PDADMAC)_3$) fusion took place much more rapidly. Thus, the film roughness played a role in bilayer formation.

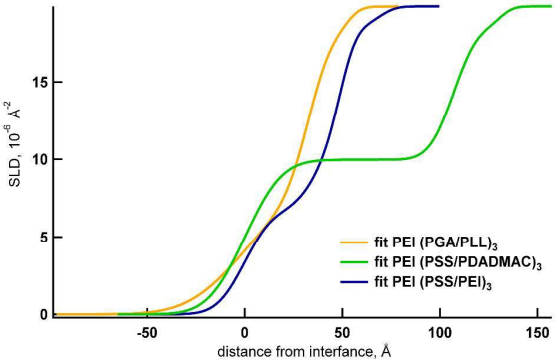

Fig. 4. Scattering length density (SLD) profiles for of $PEI(PGA/PLL)_3$, $PEI(PSS/PEI)_3$, $PEI(PSS/PDADMAC)_3$. Zero on the horizontal axis refers to the air-PEM interface.

View Article Online
DOI: 10.1039/C7SM01645J

4. Conclusions

We have investigated surface properties of polyelectrolyte multilayer films, namely PEI(PSS/PEI)n, PEI(PSS/PDADMAC)n and PEI(PGA/PLL)n that were previously used as cushions for supported lipid bilayer formation *via* surface induced fusion of POPC/POPE liposomes.[20] The contact angle of water droplets on the substrates covered with these PEMs was determined as a measure of their relative hydrophilicity/hydrophobicity. We observed that all the studied films terminated by polycation were more hydrophobic than polyanion terminated ones, which followed general phenomenon, known as odd-even effect.[33,64] $(PEI/PSS)_3$ were more hydrophobic than other polyelectrolyte multilayers studied, for both polycation terminated ($PEI(PSS/PEI)_3$) and polyanion terminated ($PEI(PSS/PEI)_3PSS$) multilayers. Moreover, PSS as an outermost layer paired with more hydrophobic PEI exhibited significantly higher contact angle than the PEM with less hydrophobic PDADMAC. This indicates the impact of the interpenetration of the oppositely charged polyions on the surface properties of the resulting PEM film.

The surface free energy (γ_S) of polyelectrolyte multilayers, determined using the Owens-Wendt approach, showed little difference in the dispersive contribution to γ_S for the studied films, independently of the top PE layer. The polar contribution to γ_S for $PEI(PSS/PEI)_3$ - either negatively or positively terminated - was much lower as compared to $PEI(PGA/PLL)_3$ and $PEI(PSS/PDADMAC)_3$. Taking into account the results for supported lipid bilayer formation on the top of these PEMs[20], we could correlate the ability of the supported lipid bilayer formation with the polar component of the surface free energy of the polyelectrolyte cushion. A lower γ_{Sp} value inhibits liposome rupture, presumably due to higher vesicle mobility at more hydrophobic, weakly interacting surfaces, resulting in bigger amount of intact vesicles adsorbed. In contrast, a higher γ_{Sp} value induces faster liposome rupture since it promotes liposome deformations, with deformed vesicles rupturing more easily due to a larger curvature around their edge.

The zeta potential determined for the PEM films terminated with polycations showed similar values. For negatively terminated PEMs, one can notice a much bigger dissimilarity in the zeta potential values depending on the type of the films studied. Surprisingly, films terminated with PSS exhibited different zeta potential values depending on the type of polycations used for the film preparation. We also observed that the zeta potential of the PEMs was not only determined by the polyelectrolyte in the terminal layer, but also depended on the whole film composition. This finding is useful and should be taken into account when polyelectrolyte multilayers are designed for a specific purpose. From the X-ray reflectivity studies on polycation-terminated PEMs, one can observe that they differ in the structure. Moreover, the roughness of the polyelectrolyte cushion could have an effect on the kinetics of liposome fusion and subsequent bilayer formation.

Our results show that combining contact angle measurements with streaming potential and XRR techniques can provide valuable insights on the physicochemical properties of polyelectrolyte multilayer films in the context of using them as cushions for biomembranes or biomolecules.

Acknowledgements

The work presented was financed by the National Science Centre, Contract No. DEC-2011/01/DST5/04913. The European Union Erasmus+ programme (project number: 2015-1-PL01-KA103-014791) is acknowledged for providing scholarship (financial support) for the research/mobility/traineeship. W.H.B. would like to acknowledge funding from the EPSRC (EP/H034862/1 and Building Global Engagement in Research (BGER)), and Marie Curie Initial Training Network (MCITN) on "Soft, Small, and Smart: Design, Assembly, and Dynamics of Novel Nanoparticles for Novel Industrial Applications" (NanoS3). XMaS is a mid-range facility supported by EPSRC (UK). We are grateful to all the beam line team staff for their support.

Notes and references

1 R. K. J. Iler, *J. Colloid Interface Sci.*, 1966, **21**, 569-594.
2 G. Decher and J. D. Hong, *Macromol. Chem. Macromol. Symp.,* 1991, **46**, 321-327.
3 G. Decher, J. D. Hong and J. Schmitt, *Thin Solid Films,* 1992, **210/211**, 831-835.
4 G. Decher, *Science*, 1997, **277**, 1232-1237.
5 G. Decher, and J. B. Schlenoff, *Multilayer Thin Films,* 2012, Wiley-VCH.
6 J. J. Richardson, J. Cui, M. Björnmalm, J. A. Braunger, H. Ejima and F. Caruso, *Chem. Rev.*, 2016, **116**, 14828-14867.
7 J. J. Richardson, M. Björnmalm and F. Caruso, *Science*, 2015, **348**, aaa2491-1-aaa2491-11.
8 A. Pajor-Swierzy, M. Kolasinska-Sojka and P. Warszynski, *Colloid. Polym. Sci.,* 2014, **292**, 455-465.
9 A. Pavlov, S. A. Gabriel, G. B. Sukhorukov and D. J. Gould, *Nanoscale*, 2015, **7**, 9686-9693.
10 J. M. Yang, R. Z. Tsai and C. C. Hsu, *Colloids Surf., B: Biointerfaces*, 2016, **142**, 98-104.
11 L. Seon, P. Lavalle, P. Schaaf and F Boulmedais, *Langmuir*, 2015, **31**, 12856-12872.
12 C. Picart, F. Caruso, J.C. Voegel and G. Decher*, Layer-by-Layer Films for Biomedical Applications,* 2014, Wiley-VCH.
13 S. L. Suib, *New and Future Developments in Catalysis: Catalysis by Nanoparticles*, Elsevier, 2013.
14 J. Borges and J. F. Mano, *Chem. Rev.,* 2014, **114**, 8883-8942.
15 M. Elzbieciak-Wodka, M. Kolasinska-Sojka, P. Nowak and P. Warszynski, *J. Electrochem. Soc.,* 2015, **738**, 195-202.
16 J. Jatschka, A. Dathe, A. Csaki, W. Fritzsche and O. Stranik, *Sensing and Bio-Sensing Research*, 2016, **7**, 62-70.
17 M. Kolasinska, R. Krastev and P. Warszynski, *J. Colloid Interface Sci.*, 2007, **305**, 46-56.
18 M. Kolasinska, R. Krastev, T. Gutberlet, and P. Warszynski, *Langmuir*, 2009, **25**, 1224-1232.
19 M. Kolasinska, R. Krastev, T. Gutberlet, and P. Warszynski, *Prog. Colloid Polym Sci.,* 2008, **134**, 30-38.
20 M. Wlodek, M. Szuwarzynski and M. Kolasinska-Sojka, *Langmuir*, 2015, **31**, 10484-10492.
21 T. Cassier, A. Sinner, A. Offenhauser and H. Moehwald, *Colloids Surf., B: Biointerfaces*, 1999**, 15**, 215-225.
22 M. Fischlechner, M. Zauling, S. Meyer, I. Estrela-Lopis, L. Cuellar, J. Irigoyen, P. Pescador, M. Brumen, P. Messner, S. Moya and E. Donath, *Soft Matter*, 2008, **4**, 2245-2258.

View Article Online
DOI: 10.1039/C7SM01645J

23 E. Reimhult, M. Zäch, F. Höök and B. Kasemo, *Langmuir*, 2006, **22**, 3313-3319.
24 E. Diamanti, D. Gregurec, M. J. Rodriguez-Presa, C. A. Gervasi, O. Azzaroni and S. E. Moya, *Langmuir*, 2016, **32**, 6263-6271.
25 M. Edvardson, S. Svedhem, G. Wang, R. Richter, M. Rodahl, and B. Kasemo, *Anal. Chem.*, 2009, **81**, 349-361.
26 J. Shao, C. Wen, M. Xuan, H. Hang, J. Frueh, M. Wan, L. Gao and Q. He, *Phys. Chem. Chem. Phys.,* 2017, **19**, 2008–2016.
27 W. He, J. C. Frueh, Z. Wu and Q. He, *ACS Appl. Mater. Interfaces*, 2016, **8**, 4407-4415.
28 X. Lin, Z. Wu, Y. Wu, M. Xuan, and Q. He, *Adv. Mater.*, 2016, **28**, 1060-1072.
29 L. Renner, T. Osaki, S. Chiantia, P. Schwille, T. Pompe and C. Werner, *J. Phys. Chem. B*, 2008, **112**, 6373-6378.
30 M. Nakamura, T. Isono and T. Ogino, *e-J. Surf. Sci. Nanotech*. 2011, **9**, 357-362.
31 R. Tero, M. Takizawa, Y. J. Li, M. Yamazaki and T. Urisu, *Langmuir*, 2004, **20**, 7526-7531.
32 Y. H. Kim, M. M. Rahman, Z. L. Zhang, N. Misawa, R. Tero, and T. Urisu, *Chem. Phys. Lett*., 2006, **420**, 569-573.
33 Z. Adamczyk, M. Zembala, M. Kolasinska and P. Warszynski, *Colloids Surf., A: Physicochem. Eng. Aspects*, 2007, **302**, 455-460.
34 M. Kolasinska and P. Warszynski, *Bioelectrochemistry*, 2005, 66, 65-70.
35 S. Wu, *J. Adhes.* 1973, **5**, 39-55.
36 C. J van Oss, M. K. Chaudhury and R. J. Good, *Chemical Review*, 1988, **88**, 927-940.
37 D. H. Kaelble, *J. Adhes.,* 1970, **2**, 66-81.
38 D. Owens and R. Wendt, *J. Appl. Polym. Sci.,* 1969, **13**, 1741-1747.
39 W. Rabel, Einige Aspekte der Benetzungstheorie und ihre Anwendung auf die Untersuchung und Veränderung der Oberflächeneigenschaften von Polymeren. Farbe und Lacke 1971, 77, 997-1005.
40 F. M. Fowkes, *Ind. Eng. Chem.,* 1964, **56**, 40-52.
41 M. Gai, J. Frueh, A. Girard-Egrot, S. Rebaud, B. Doumeche and Q. He, *RSC Adv.*, 2015, **5**, 51891-51899.
42 R. Kugler and W. Knoll, *Bioelectrochemistry*, 2002, **56**, 175-178.
43 R. Mészáros, L. Thompson, M. Bos and P. De Groot, *Langmuir*, 2002, **18**, 6164-6169.
44 S. Schwarz, K. J. Eichhorn, E. Wischerhoff and A. Laschewsky, *Colloids Surf., A: Physicochem. Eng. Aspects,* 1999, **159**, 491-501.
45 R. A. van Wagenen and J. D. Andrade, J. *Colloid Interface Sci.*, 1980, **76**, 305-314.
46 P. J. Scales, F. Grieser and T. W. Healy, *Langmuir*, 1990, **6**, 582-589.
47 Z. Adamczyk, M. Zembala, P. Warszynski and B. Jachimska, *Langmuir*, 2004, **20**, 10517-10525.
48 M. Zembala and Z. Adamczyk, *Langmuir*, 2000, **16**, 1593-1601.
49 M. Zembala and P. Dejardin, *Colloids Surf., B: Biointerfaces*, 1994, **3**, 119-129.
50 Z. Adamczyk, M. Zembala and A. Michna. *J. Colloid Interface Sci.*, 2006, **303**, 353-364.
51 W. Norde and E. Rouwendal. *J. Colloid Interface Sci.,* 1990, **139**, 169-176.
52 A. V. Elgersma, R. L. J. Zsom, J. Lyklema and W. Norde, *J. Colloid Interface Sci.,* 1992, **152**, 410-428.
53 M. Wasilewska and Z. Adamczyk, *Langmuir*, 2011, **27**, 686-696.
54 F. Speranza, G. A. Pilkington, T. G. Dane, P. T. Cresswell, P. X. Li, R. M. J. Jacobs, T. Arnold, L. Bouchenoire, R. K. Thomas, and W. H. Briscoe, *Soft Matter*, 2013, **9**, 7028-7041.
55 W. H. Briscoe, F. Speranza, P. Li, O. Konovalov, L. Bouchenoire, J. v Stam, J. Klein, R. M. J. Jacobs and R. K. Thomas, *Soft Matter*, 2012, **8**, 5055-5068.
56 M. Zenkiewicz, *J. Achiev. Mater. Manuf. Eng.*, 2007, 24, 137-145.
57 B. Sironi, T. Snow, C. Redeker, A. Slastanova, O. Bikondoa, T. Arnold, J. Klein, and W.H. Briscoe, *Soft Matter*, 2016, **12**, 3877-87.
58 A. Nelson, *J. Appl. Cryst.*, 2006, **39**, 273-276.
59 M. C. Hsieh, R. J. Farris and T. J. McCarthy, *Macromolecules*, 1997, **30**, 8453-8458.
60 M. Kolasinska and P. Warszynski, *Appl. Surface Sci.*, 2005, **252**, 759-765.
61 T. Isono, H. Tanaka and T. Ogino, *e-J. Surf. Sci. Nanotech.,* 2007, **5**, 99-102.
62 C. Alvarez-Lorenzo and A. Concheiro, *Current Opinion in Biotechnology*, 2013, **24**, 1167-1173.
63 M. Kolasinska-Sojka, M. Wlodek, M. Szuwarzynski, S. Kereiche, L. Kovacik and P. Warszynski, *Colloids Surf. B, Biointerfaces,* 2017, **158**, 667-674.
64 P. Nestler, S. Block and C. A. Helm, *J. Phys. Chem. B*, 2011, **116**, 1234-1243.